

Comparison Study of PHBA-intercalated Mg/Al-LDH and PHBA-immobilized Mg/Al-LDH: Characterization and Application for $[\text{AuCl}_4]^-$ Removal from Solution

Lutfi Aditya Hasnowo^{1*}, Sri Juari Santosa², Bambang Rusdiarso²

¹Department of Nuclear Chemical Engineering, Polytechnic Institute of Nuclear Technology, Yogyakarta, Indonesia.

²Department of Chemistry, Faculty of Mathematic and Natural Science, Universitas Gadjah Mada, Yogyakarta, Indonesia

*Corresponding Author: lutfi.aditya@batan.go.id

Abstract

Synthesis of *p*-hydroxybenzoic acid (PHBA)-intercalated Mg/Al-LDH and PHBA-immobilized Mg/Al-LDH had been conducted. PHBA-intercalated Mg/Al-LDH hybrid was synthesized by co-assembly process of Mg/Al-LDH nanosheets and PHBA anions. PHBA-immobilized Mg/Al-LDH was prepared by indirect synthesis, where PHBA anions were attached on surface of the Mg/Al-LDH material. X-ray Diffraction result showed that the PHBA-intercalated Mg/Al-LDH hybrid has the lattice parameter of $a=3.02 \text{ \AA}$, $c=46.77 \text{ \AA}$ and basal spacing $d_{003}=15.14 \text{ \AA}$, where PHBA has been intercalated in interlayer of the hybrid. The PHBA-immobilized Mg/Al-LDH has lattice parameter of $a=3.06 \text{ \AA}$, $c=23.70 \text{ \AA}$ and basal spacing $d_{003}=7.90 \text{ \AA}$. The result confirmed that PHBA attached on surface of the hybrid for PHBA-immobilized Mg/Al-LDH. The optimum 10 mL of $[\text{AuCl}_4]^-$ 100 mg L⁻¹ removal condition of both hybrids were reached at pH 3. The optimum interaction time of $[\text{AuCl}_4]^-$ and PHBA-intercalated Mg/Al-LDH hybrid was 250 minutes, respectively, while that for $[\text{AuCl}_4]^-$ and PHBA-immobilized Mg/Al-LDH was 150 minutes. Removal of $[\text{AuCl}_4]^-$ by PHBA-intercalated Mg/Al-LDH hybrid followed pseudo second order kinetic, whereas by PHBA-immobilized Mg/Al-LDH followed pseudo first order kinetic. Characterization using stereo photomicroscope confirmed that $[\text{AuCl}_4]^-$ could be reduced to Au metal by both hybrids.

Keywords: Layered double hydroxide, *p*-hydroxybenzoic acid, hybrid material, $[\text{AuCl}_4]^-$ removal

Abstrak (Indonesian)

Telah dilakukan sintesis material hibrida Mg/Al-LDH terinterkalasi asam para hidroksibenzoat (APHB) dan Mg/Al-LDH terimobilisasi APHB serta penerapannya untuk penghilangan $[\text{AuCl}_4]^-$ dari larutan. Mg/Al-LDH terinterkalasi APHB disintesis melalui proses co-assembly nanosheet Mg/Al-LDH dan APHB. Mg/Al-LDH terimobilisasi APHB disintesis secara tidak langsung dimana APHB diadsorpsikan pada material Mg/Al-LDH. Hasil menunjukkan hibrida Mg/Al-LDH terinterkalasi APHB mempunyai nilai parameter kisi a , c dan basal spacing d_{003} masing-masing sebesar 3,02; 46,77; dan 15,14 Å, dimana APHB berada di daerah antar lapis hibrida. Nilai parameter kisi a , c dan basal spacing d_{003} hibrida Mg/Al-LDH terimobilisasi APHB masing-masing 3,06; 23,70; dan 7,90 Å, dimana APHB berada di permukaan luar lapisan hibrida. Penghilangan 10 mL larutan $[\text{AuCl}_4]^-$ 100 mg/L oleh 10 mg kedua material optimum pada pH 3 dan waktu kontak 250 menit untuk Mg/Al-LDH terinterkalasi APHB, sedangkan pada Mg/Al-LDH terimobilisasi APHB optimum pada pH 3 dan waktu kontak 150 menit. Penghilangan $[\text{AuCl}_4]^-$ oleh material Mg/Al-LDH terinterkalasi APHB mengikuti kinetika pseudo orde kedua, sedangkan oleh material Mg/Al-LDH terimobilisasi APHB mengikuti pseudo orde pertama. Hasil fotomikroskop stereo menunjukkan bahwa $[\text{AuCl}_4]^-$ telah tereduksi oleh kedua hibrida menjadi logam Au.

Kata Kunci: Hidroksida ganda terlapis, asam *p*-hidroksibenzoat, material hibrida, penghilangan $[\text{AuCl}_4]^-$

Article Info

Received 17 August 2020

Received in revised 7

September 2020

Accepted 8 September 2020

Available online 20 October 2020

INTRODUCTION

In recent, Layered Double Hydroxides (LDH) have attracted a great attention because of their layered structure and high anion exchange capacity, which can make various technical applications [1-4]. LDH compounds are a class of anionic clays which can be represented by the general formula of $[M^{2+}_{1-x}M^{3+}_x(OH)_2]^{x+}[A^{n-}]_{x/n} \cdot mH_2O$, where M^{3+} and M^{2+} are tri- and divalent metal ions, and A^{n-} is the exchangeable anions [5-7]. LDH compounds are the only known inorganic materials with positive layer charge, their structural units are made from stacks of positively charged octahedral sheets of $([M^{2+}_{1-x}M^{3+}_x(OH)_2]^{x+})$ and the corresponding anions (A^{n-}) as well as water molecules. The positive charge is due to substitution of M^{2+} with M^{3+} in the brucite-like metal hydroxide $M(OH)_2$ and is balanced by the negative charge (A^{n-}) from the interlayer anions. Meanwhile, various amounts of water (mH_2O) are hydrogen bonded to the hydroxide layers or to the interlayer anions, forming the 3D layered structure [7,8].

There are increasing interests in using LDHs, because of their utilization as adsorbent. LDH potentially have high capability for adsorption. LDH's adsorption ability is supported by their high anion exchange and surface area [9,10]. In order to enhance the effectiveness of their adsorption capability, many researchers have modified LDHs by various ways. There are some LDH modification techniques, but surfaces and galleries modifications were more often conducted.

In the LDH structure, some of the M^{2+} ions are replaced by M^{3+} ions, resulting in positively charged layers [9]. Although this charge is compensated by interlayer anions, the layer surface of the LDH can still electrostatically interact with negatively charged foreign species, so, a modifier can be immobilized on the LDH surface. On the other hand, LDH can also as hosts for nanoscale reactions especially remarked as a template for the creation of intercalated supramolecular arrays [11,12].

Many different anions can be intercalated into the interlayer space, and their species can vary to cater to different needs. As for the diversity of organic materials and their particular structural features, organic anion intercalated LDH have aroused peculiar interest [12].

As adsorbent, LDH modifications are not only to enhance the adsorption capability but also can appear new properties of the LDH. Selection of substance to be a modifier is important because it is tailored to the desired final capability of the composite material. *p*-hydroxybenzoic acid (PHBA) is a benzoic acid

derivative which has a hydroxyl (-OH) group bound to the aromatic ring. The presence of a hydroxyl group on PHBA causes it can be a reductor. PHBA has a reduction potential value of -0.5037 V.

PHBA study as a reducing agent was conducted by Maghfiroh (2015), where PHBA was used as a reducing agent for $AgNO_3$ to $Ag(0)$ [13]. The result showed that PHBA was the best reductor in reducing $Ag(I)$ to $Ag(0)$ compared to ortho hydroxybenzoic acid and gallic acid. The reduction potential value of $Ag(I)$ is +0.8000 V while $[AuCl_4]^-$ is +1.002 V [14]. The reduction potential value of $[AuCl_4]^-$ is more positive than $AgNO_3$, so that it is expected that $[AuCl_4]^-$ can be reduced more easily by PHBA.

The synthesis of two types of compounds, namely Mg/Al-LDH and PHBA, is expected to form a new hybrid material which has a double ability in the removal process $[AuCl_4]^-$. This new hybrid material can not only adsorb but can also reduce $[AuCl_4]^-$ to Au metal.

In this study, PHBA-intercalated Mg/Al-LDH hybrid material was synthesized and then used for the removal process $[AuCl_4]^-$ in solution. Before being intercalated by PHBA, Mg/Al-LDH nanosheet was synthesized first with a "bottom-up" approach through an alternative co-precipitation method. The formed Mg/Al-LDH was then intercalated by PHBA via co-assembly process. In addition, the synthesis of PHBA-immobilized Mg/Al-LDH hybrid material was also carried out as a comparative hybrid material. PHBA-immobilized Mg/Al-LDH hybrid material was synthesized through indirect synthesis. The application of the two hybrid materials, namely PHBA-intercalated Mg/Al-LDH and PHBA-immobilized Mg/Al-LDH in the removal process $[AuCl_4]^-$ in solution was studied by determining the effect of pH of solution and interaction time.

MATERIALS AND METHODS

Materials

All chemicals - $Mg(NO_3)_2 \cdot 6H_2O$, $Al(NO_3)_3 \cdot 9H_2O$, NaOH, and HCl were purchased from Merck Co. Inc., Germany, $NH_3 \cdot H_2O$ and *p*-hydroxybenzoic acid were purchased from Sigma-Aldrich and nitrogen sufficiently high purity (99.99%) was purchased from CV Perkasa (Indonesia) - are of analytical grade and used as received without further purification. $[AuCl_4]^-$ solution ($HAuCl_4$) was prepared by dissolving of gold (99.99%) in aqua regia solution. Gold (99.99%) were purchase from PT. ANTAM Indonesia.

Synthesis process

A two-step process was performed to synthesize the target samples. In the first step, Mg/Al-LDH

nanosheets were synthesized as follows [15] A mixture of salts ($Mg^{2+} + Al^{3+}$) 0.3 mol/L with a molar ratio of 2:1 was prepared by 1.026 g (4 mmol) $Mg(NO_3)_2 \cdot 6H_2O$ and 0.750 g (2 mmol) $Al(NO_3)_3 \cdot 9H_2O$ dissolved in CO_2 free distilled water 20 mL. An alkali solution (~7 wt%) was prepared by diluting $NH_3 \cdot H_2O$ solution (25 wt%) with water. These two solutions were injected into the T type microchannel reactor through two inlets using a peristaltic pump, each at a flow rate of 20 mL/min. Furthermore, the resulting suspension was collected at the reactor outlet and filtered by Millipore 0.8 μm to remove the supernatant. The precipitate was washed three times with distilled water by re-dispersion, yielding gel-like Mg/Al-LDH nanosheets.

In the second step, 50 mL of 1,0 mmol PHBA solution was added dropwise into 50 mL of 100 g/L Mg/Al-LDH nanosheets dispersion under continuous stirring at room temperature for 12 h. In the tests, the pH in the starting mixtures was set at 8. The suspension was centrifuged and filtered with Millipore 0.8 μm . The precipitate was washed by aquadest and dried at room temperature to yield a PHBA-Intercalated Mg/Al-LDH hybrid material.

In addition, PHBA-immobilized Mg/Al-LDH hybrid material was synthesized through indirect synthesis. First, a pristine Mg/Al-LDH in bulky state (three dimension) was prepared by the typical coprecipitation method. Amount of 12.821 g (0.05 mol) $Mg(NO_3)_2 \cdot 6H_2O$ and 9,378 g (0.025 mol) $Al(NO_3)_3 \cdot 9H_2O$, were dissolved in 100 mL of distilled water. NaOH 0.5 M was added dropwise to the solution until reaches pH 10. The resulting solution was continued with stirring for 30 under N_2 atmosphere. The mixture was then hydrothermally treated at 120°C for 5 hours. The suspension was filtered, washed and then dried at 70°C until constant weight was achieved, yielding pristine Mg/Al-LDH.

Then, 0,01 g of pristine Mg/Al-LDH was interacted with 10 mL of 100 mg/L PHBA solution. In the tests, the pH in the starting mixtures was set at 8 and then the mixture was shaken for 90 min. After being shaken, the dispersion was filtered through Whatman filter and the remaining PHBA in the filtrate was determined spectroscopically using UV-Vis spectrophotometer at a wavelength giving maximum absorption.

Characterization

X-ray diffraction (XRD) patterns of the prepared samples were recorded by Shimadzu-6000. Fourier transform infrared spectroscopy (FT-IR) spectra of the samples were collected using Fourier transformation infrared spectroscope (Nicolet Avatar 360IR) in

reflectance mode, and in the range 400-4000 cm^{-1} . The morphology and content analysis of materials were observed by Scanning Electron Microscopy (JEOL JSM-6510LA), and Particles size of the sample were estimated by Particle Size Analyzer (Horiba SZ-100). Atomic Absorption Spectroscopy (AAS, ContrAA 300) for Au(III) content analysis, and Stereo Microscopy (Nikon Digital Camera DXm 1200C to identify Au(0). Ultraviolet-visible spectrophotometer (UV-Vis, Shimadzu UV-1800 pharmaspec).

Effect of medium acidity on reductive adsorption of $[AuCl_4]^-$

Ten milligram of PHBA-intercalated Mg/Al-LDH was added into every 10 mL of $[AuCl_4]^-$ 100 mg/L solutions at pH 2, 3, 5, 7, 9 and 11. The mixed solutions were then stirred for 90 min, filtered and the remaining $[AuCl_4]^-$ in the filtrate was determined using AAS. As a comparison, the same experiment was conducted for PHBA-immobilized Mg/Al-LDH.

Effect of interaction time on reductive adsorption of $[AuCl_4]^-$

Into a series of flasks containing 10 mL of $[AuCl_4]^-$ 100 mg/L solutions at optimum pH obtained from the above experiment, 10 mg of PHBA-intercalated Mg/Al-LDH was added. The flasks were then subjected to continuous stirring at contact times 0, 10, 20, 30, 60, 90, 120, 150, 200, 250, 300 and 350 min. At each selected contact time, a sample from the respective flask was immediately taken, filtered through a Whatman 42 filter and the remaining concentration of $[AuCl_4]^-$ in the filtrate was analyzed by AAS. The same experiment was repeated but instead of PHBA-immobilized Mg/Al-LDH was used.

Stability of p-hydroxybenzoic acid on Mg/Al-LDH

To test the stability of the PHBA-intercalated Mg/Al-LDH and PHBA-immobilized Mg/Al-LDH, it was necessary to test the desorption of the two hybrid materials into 10 mL of distilled water by adjusting the pH variation of distilled water. The pH of the distilled water was adjusted to variations of pH 2, 3, 5, 7, 9, and 11. 0.010 g of each hybrids material was added to each aquadest which had been adjusted and then shaken it for 90 minutes. After separating supernatant from the solid, the content of dissolved PHBA in supernatant was determined spectroscopically at wavelength giving maximum absorption.

RESULTS AND DISCUSSION

XRD analysis

The XRD pattern results show that all formed materials were layered materials. This was indicated by the appearance of Bragg Mg/Al-LDH diffraction peaks

clearly in low-angle range [14]. In addition, there was also a diffraction peak (110) at 2θ angle 61° in all of these materials. This peak was characteristic of lattice a parameter. The clear difference seen in Figure 1 was that there were shifts in basal spacing d_{003} of the two hybrid materials than pristine Mg/Al-LDH. Based on Table 1, there was a decrease in basal spacing d_{003} of PHBA-immobilized Mg/Al-LDH although it was not too significant, i.e. from 8.11 \AA to 7.90 \AA . Based on these data it could be said that PHBA was only on the surface of PHBA-immobilized Mg/Al-LDH and did not enter the inter-layer area. The reduction in basal spacing d_{003} Mg/Al-LDH was possible because PHBA has hydrophilic properties which makes it able to interact well with H_2O . This could be the driving force of the PHBA to attract H_2O molecules in the inter-layer area thereby reducing the basal spacing value d_{003} Mg/Al-LDH.

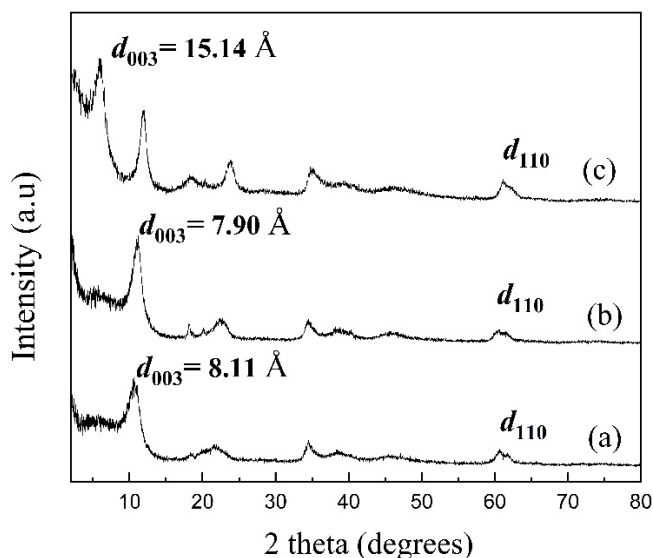


Figure 1. Powder XRD pattern of (a) Mg/Al-LDH, (b) PHBA-intercalated Mg/Al-LDH, and (c) PHBA-immobilized Mg/Al-LDH

A different phenomenon was seen in the PHBA-intercalated Mg/Al-LDH. The peak shift occurred towards a smaller angle than pristine Mg/Al-LDH indicating PHBA anion had entered to the area between the Mg/Al-LDH layers. This was due to the size of the molecular diameter of the PHBA anion which was larger than the NO_3^- and the H_2O molecules which should fill the area between layers of Mg/Al-LDH. Based on theory we could estimate the size of the inter-layer distance (basal spacing value d_{003} = the thickness of the Mg/Al-LDH layer + the size of the distance between the Mg/Al-LDH regions). The thickness of the Mg/Al-LDH layer is the average distance between hydroxide to hydroxide in different fields in the brucite

like layer, which is 4.70 \AA [16]. According to the size of the distance between layers of the synthesized material was 10.44 \AA (PHBA-intercalated Mg/Al-LDH) and 3.20 \AA (PHBA-immobilized Mg/Al-LDH). The measurement of the distance between the layers could be used as an indication that the PHBA anion measuring 6.35 \AA has entered to the galleries area of the PHBA-intercalated Mg/Al-LDH. Whereas in the PHBA-immobilized Mg/Al-LDH material, PHBA was only on the surface and did not enter the interlayer area.

Table 1. Lattice parameter values of the materials

Material	d_{003} (\AA)	c (\AA)	a (\AA)
PHBA-intercalated Mg/Al-LDH	15.14	46.77	3.02
PHBA-immobilized Mg/Al-LDH	7.90	23.70	3.06
Mg/Al-LDH	8.11	24.33	3.06

Mg/Al-LDH has a unit cell structure in the form of rhombohedral $R-3m$ with an octahedral system [17], where the a and c lattice parameter values of the material can be found from the basal spacing d_{003} and d_{110} basal spacing values. The two XRD diffractograms showed the appearance of diffraction peaks (110) at an angle of 2θ which was not much different, namely 61.35° (PHBA-intercalated Mg/Al-LDH) and 60.29° (PHBA-immobilized Mg/Al-LDH). The position of the diffraction peak (110) can indicate the lattice parameter value of the Mg/Al-LDH material, where lattice parameter $a = 2d_{110}$, so that the lattice parameter a of each material is 3.02 \AA (PHBA-intercalated Mg/Al-LDH) and 3.06 \AA (PHBA-immobilized Mg/Al-LDH).

The lattice parameter a on Mg/Al-LDH material shows the distance between two adjacent hydroxide groups on the same side of the layer or shows the distance between the closest metal ions present in the Mg/Al-LDH layer. Information on the c lattice parameters of the two materials can be obtained from the basal spacing value d_{003} , where the lattice parameter $c = 3d_{003}$, so that the value of the c lattice parameter of PHBA-intercalated Mg/Al-LDH and PHBA-immobilized Mg/Al-LDH are respectively 46.42 \AA and 23.70 \AA . The lattice parameter c in Mg/Al-LDH shows the same layer-dependent distance in rhombohedral $R-3m$ unit structure.

FT-IR analysis

FTIR spectra for the two hybrid materials in comparison with pristine Mg/Al-LDH were illustrated in Figure 2. Peaks around 447.32 cm^{-1} was found in all samples associated with Mg-O-Al bonds. Several other absorption peaks below 1000 cm^{-1} also appeared to be

associated with Mg-OH and Al-OH bond [18]. Figure 2 showed decrease in absorption peaks in 3447.18 cm^{-1} which shows reduction in the hydroxyl group on the surface of Mg/Al-LDH and from H_2O molecules found in the inter-layer region. These indicated that adsorption has occurred on the surface of Mg/Al-LDH so that the amount of -OH was decreased. Reduction of absorption peak intensity also occurred in overtone absorption of nitrate ions at wave number 1383 cm^{-1} which is expected to be a change in nitrate ions which might have been protonated into nitric acid which dissolve in water [19].

Figure 2 also shows the emergence of new peaks at several wavenumber. FT-IR spectra for two hybrid materials showed the existence of functional groups of the hydroxybenzoic acids, such as the absorption peaks at wave numbers around 1541 and 1612 cm^{-1} , which were respectively the aromatic ring C-C stretching and the R-COO asymmetrical stretching vibration of the PHBA. At 1169 cm^{-1} was also recorded absorption peak which estimated to be a C-O stretching vibration from the PHBA.

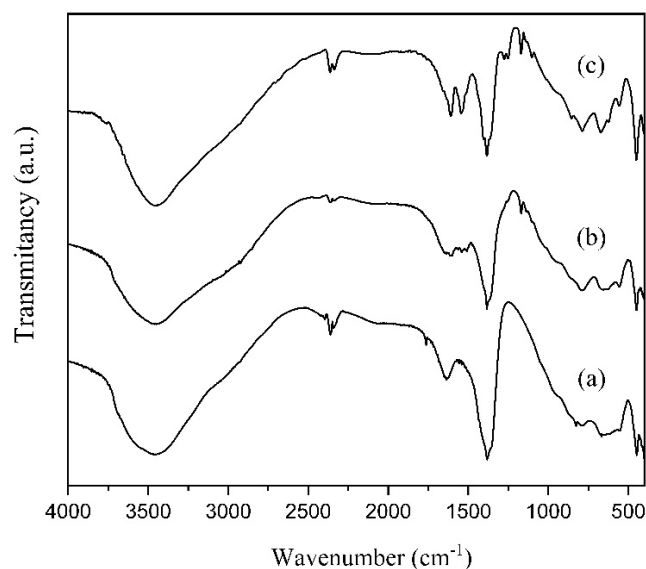


Figure 2. FT-IR pattern of (a) Mg/Al-LDH, (b) PHBA-intercalated Mg/Al-LDH, and (c) PHBA-immobilized Mg/Al-LDH

The difference in absorption peak intensity between the two hybrid materials appears in wave numbers around 1383 and 3448 cm^{-1} . The absorption peak around wavenumber 1384 cm^{-1} was N-O stretching vibration of the NO_3 anion that was in the intergroup area of Mg/Al-LDH, while the wave number around 3447 cm^{-1} was the OH stretching vibration of the hydroxy group at surface (layer plane) Mg/Al-LDH and water molecules that exist in the inter-layer area. The difference in absorption peak

intensity occurred because in PHBA-intercalated Mg/Al-LDH material there was a change of species in the inter-layer area where nitrate and molecular anions were replaced by PHBA anions, so the intensity which was characteristic of nitrate anions and H_2O molecules has a significant decrease [20-22].

In PHBA-immobilized Mg/Al-LDH, PHBA anion was only on the surface (plane layer) of Mg/Al-LDH, so that there were still many nitrate anions and H_2O molecules in the inter-layer area. The difference in intensity was also seen at the peak of absorption at wave numbers around 1542 and 1612 cm^{-1} , which were respectively the aromatic ring C-C stretching absorption and the R-COO asymmetry stretching vibration of the PHBA anion.

In PHBA-intercalated Mg/Al-LDH, there were atomic absorptions at around 1276 and 1252 cm^{-1} which were C-O stretching vibrations from carboxylic groups and COH bending vibrations of phenol groups from PHBA, whereas in hybrid Mg / Al-LDH materials immobilized PHBA did not appear. This showed that the PHBA anion has interacted more in the PHBA intercalated Mg/Al-LDH hybrid material than in the PHBA-immobilized Mg /Al-LDH. In both materials was visible peaks peak at wave numbers around 1170 cm^{-1} estimated to be a vibration stretching C-O phenol group from PHBA [21-23].

Stability of *p*-hydroxybenzoic acid on PHBA-intercalated Mg/Al-LDH and PHBA-immobilized Mg/Al-LDH

Figure 3 shows the stability of PHBA-intercalated on Mg/Al-LDH at various pH mediums. Stability of the intercalated PHBA towards dissolution was excellent from pH 3.0 to 9.0, i.e. at the level $99.36 \pm 0.33\%$. In mediums with extreme acidity and alkalinity levels, stability of PHBA on Mg/Al-LDH was degraded to the value 89.72 and 89.27 % at pH 2.0 and 11.0, respectively. In the case of immobilized PHBA, its stability was $95.99 \pm 3.04\%$ in the pH range 3.0 to 9.0 and then it degraded to the value 40.15 and 51.67 % at pH 2.0 and 11.0.

At the high acidity level of the medium, the hydroxyl group of the hybrid was protonated and the metal bonds were broken so that the metal cations dissolve. The dissolution of the cations was also accompanied by the release of PHBA in solution. While at high alkalinity level (pH 11), the released APHB was relatively high. This is because at high alkalinity level, amount of OH^- anion classified as a hard base in the solution is in large amounts, so that the cations Mg^{2+} and Al^{3+} classified as hard acids will prefer to interact with OH^- anion than PHBA anion.

This results in the PHBA anions being depleted in solution.

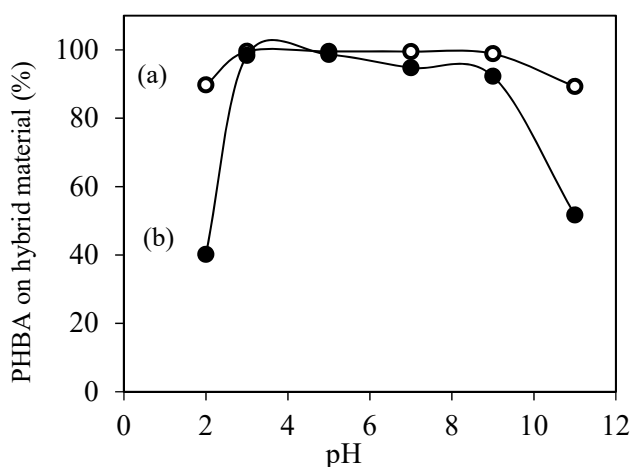


Figure 3. Effect of pH to stability of (a) PHBA-intercalated Mg/Al-LDH and (b) PHBA-immobilized Mg/Al-LDH

This result showed that PHBA-intercalated Mg/Al-LDH was relatively more stable than PHBA-immobilized Mg/Al-LDH. This phenomenon occurred because in PHBA-intercalated Mg/Al-LDH, PHBA was dominant in the gallery and was protected by Mg/Al-LDH as the material host.

Effect of medium acidity on reductive adsorption of $[\text{AuCl}_4]^-$

Figure 4 shows that medium acidity greatly affects the removal of $[\text{AuCl}_4]^-$ by PHBA-intercalated Mg/Al-LDH and PHBA-immobilized Mg/Al-LDH. At high acidity levels of the medium (pH 2), the removal ability of $[\text{AuCl}_4]^-$ by two hybrid materials was very low, because in pH under, the hydroxyl group of the two materials was protonated and Mg or Al bonds were broken so that the metal cations dissolve. The dissolution of the cations was also accompanied by the release of PHBA in solution, resulting in a low removal of $[\text{AuCl}_4]^-$.

$[\text{AuCl}_4]^-$ optimum removal occurs at medium pH 3. The higher the pH value, the lower the removal of $[\text{AuCl}_4]^-$ by the materials. This was related to the pH_{pzc} Mg/Al-LDH value reported by Martin et al (1999) was 12, so that at pH conditions 3 to 11, the positive charge level on Mg/Al-LDH tended to decrease, resulting in adsorption of $[\text{AuCl}_4]^-$ charged negative decreases [23]. $[\text{AuCl}_4]^-$ was dominant at pH lower than 4.5 and gradually changes to $[\text{Au}(\text{OH})_4]^-$ with the increasing pf pH [24-26].

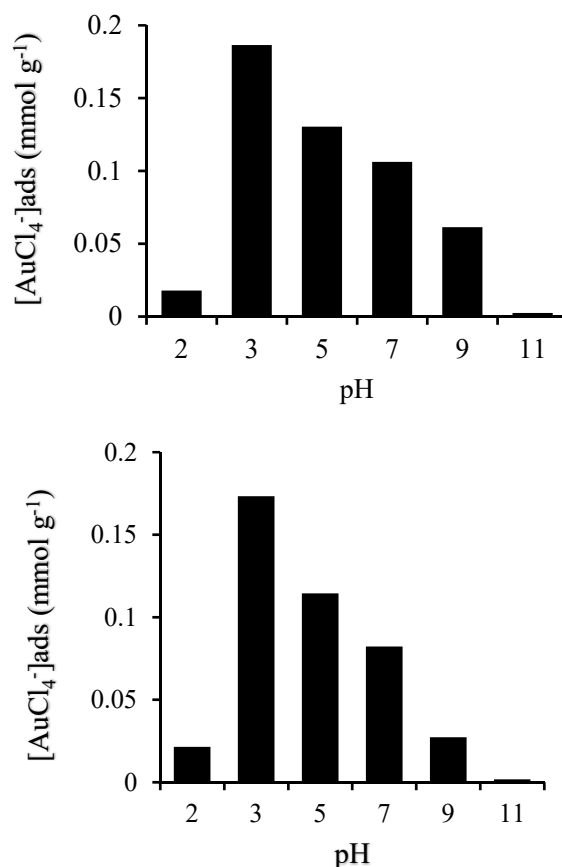


Figure 4. Effect of medium acidity on reductive adsorption of $[\text{AuCl}_4]^-$ by PHBA-intercalated Mg/Al-LDH and PHBA-immobilized Mg/Al-LDH

In the medium pH 3 gold was dominant as $[\text{AuCl}_4]^-$, so the $[\text{AuCl}_4]^-$ removal process can take place optimally. In addition, in process of removal of $[\text{AuCl}_4]^-$ by two hybrid materials were also reduction process in $[\text{AuCl}_4]^-$. The OH group of the hydroxybenzoic acid present in the material plays a role in reducing $[\text{AuCl}_4]^-$ to Au(0) and also did not rule out the OH group also played a role in the adsorption process $[\text{AuCl}_4]^-$. In the reductive adsorption process of $[\text{AuCl}_4]^-$, OH group in PHBA which was presented in Mg/Al-LDH was predicted to undergo oxidation. This phenolic compound when oxidized would produce a quinone [27-29].

Kinetic study of AuCl_4^- removal

The ability of PHBA intercalated Mg/Al-LDH and PHBA immobilized Mg/Al-LDH to remove $[\text{AuCl}_4]^-$ was carried out at temperature 25°C and initial medium acidity equivalent to pH 3. To describe adsorption data obtained under non-equilibrium conditions, two kinetic models, namely the pseudo-first-order (PFO) and the pseudo-second-order (PSO)

were used [28-33]. The kinetic rate equations following PFO can be represented as:

$$\frac{dq_t}{dt} = k_1(q_e - q_t) \tag{1}$$

Where k_1 is the rate constant.

Integrating Eq. (1) for boundary conditions $t = 0$ and $t = t$ and $q_t = 0$ and $q_t = q_t$, gives [32]:

$$\log(q_e - q_t) = \log(q_e) - \frac{k_1}{2,303} t \tag{2}$$

The constants can be determined experimentally by plotting of $\log(q_e - q_t)$ against t .

Likewise, the reductive adsorption of $[\text{AuCl}_4]^-$ following PSO kinetics can be represented as

$$\frac{dq_t}{dt} = K_2(q_e - q_t)^2 \tag{3}$$

Where k_2 is the rate constant.

Integrating Eq. (3) for boundary conditions $t = 0$ and $t = t$ and $q_t = 0$ and $q_t = q_t$, gives [33]:

$$q_t = \frac{k_2 q_e^2 t}{1 + k_2 q_e t} \tag{4}$$

Eq. (4) can be linearized to linear forms as

$$\frac{t}{q_t} = \frac{1}{k_2 q_e^2} + \frac{1}{q_e} t \tag{5}$$

The constants can be determined experimentally by plotting of t/q_t against t .

Based on the results of the experiment shown in Figure 5, the equilibrium of removal of $[\text{AuCl}_4]^-$ by PHBA-intercalated Mg/Al-LDH and PHBA-immobilized Mg/Al-LDH occurred at 250 and 150 minutes, respectively. Although their ability to remove $[\text{AuCl}_4]^-$ is different from one another, the profiles of removal of $[\text{AuCl}_4]^-$ by the two hybrid materials are similar. The removal of $[\text{AuCl}_4]^-$ by the two adsorbents was initially rapid and began to slow down from the contact time of about 35 minutes. Rate constant of PFO and PSO for the removal of $[\text{AuCl}_4]^-$ by PHBA-intercalated Mg/Al-LDH and PHBA-immobilized Mg/Al-LDH is shown in Table 2.

Interestingly, it was observed that the R^2 value of the PFO from PHBA-immobilized Mg/Al-LDH was higher than and PHBA-intercalated Mg/Al-LDH, whereas the opposite trend prevailed for PSO. As previously thought, the number of PHBA in PHBA-intercalated Mg/Al-LDH material was more than in PHBA-immobilized Mg/Al-LDH. So, the number of active sites for $[\text{AuCl}_4]^-$ increased. On the other hand, as previously indicated, PFO will prevail in conditions where the initial adsorbate concentration is much higher than the number of available adsorbent active sites [34-38].

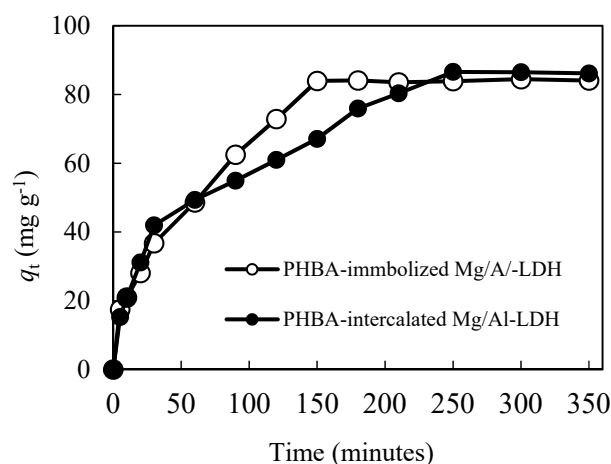


Figure 5. Effect of time on reductive adsorption of $[\text{AuCl}_4]^-$ by PHBA-intercalated Mg/Al-LDH and PHBA-immobilized Mg/Al-LDH

Therefore, increasing the available active sites from PHBA-immobilized Mg/Al-LDH to PHBA-intercalated Mg/Al-LDH could exacerbate the predominance of $[\text{AuCl}_4]^-$ concentration over the number of active sites available and consequently the application of a PFO kinetics model as shown by the value of R^2 was degraded while PSO kinetics model increased.

Table 2. Caption of table rate constant of PFO and PSO for the removal of $[\text{AuCl}_4]^-$ on PHBA-intercalated Mg/Al-LDH and PHBA-immobilized Mg/Al-LDH

No.	Kinetic Model	PHBA-intercalated Mg/Al-LDH	PHBA-immobilized Mg/Al-LDH
1.	Pseudo-first-order (PFO)		
	$k_1 (10^{-2} \text{ min}^{-2})$	1.0364	1.5199
	R^2	0.9593	0.9827
2.	Pseudo-second-order (PSO)		
	$k_1 (10^{-4} \text{ g/mg min})$	3.2778	3.3522
	R^2	0.9596	0.9104

The presence of Au (0) as a result of reduction process $[\text{AuCl}_4]^-$ by PHBA-intercalated Mg/Al-LDH and PHBA-immobilized Mg/Al-LDH could be known by comparing the visual appearance of the two hybrid materials between before and after the removal process $[\text{AuCl}_4]^-$ using a stereo photomicroscope as shown by Figure 6. Figure 6 (a) and (c) it could be observed that before the removal process of $[\text{AuCl}_4]^-$, the surface of the two hybrid materials was pure white. In Figure 6 (c) and (d) it shows that Au metal has been formed which was seen in the stereo microscope photo as a shiny part covering the surface of the hybrid material

which turns brown. The shiny color that occurs was the reflection of the microscope light hitting the gold metal surface [39]. This was because gold is a metal that has shiny physical properties, making it more shining when exposed to light.

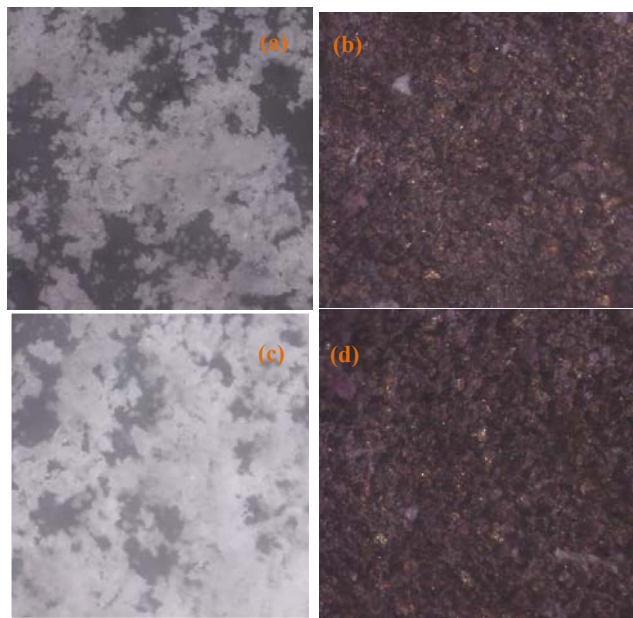


Figure 6. Stereo photomicroscope zoom 100x of PHBA-intercalated Mg/Al-LDH (a) before $[\text{AuCl}_4]^-$ removal (b) after $[\text{AuCl}_4]^-$ removal, and PHBA-immobilized Mg/Al-LDH (c) before $[\text{AuCl}_4]^-$ removal (d) after $[\text{AuCl}_4]^-$ removal

CONCLUSION

Intercalation of PHBA to the interlayer area of Mg/Al-LDH was successfully done, identified through FTIR spectroscopy that there was the presence of C-C aromatic ring stretching vibrations, C-O stretching vibrations of carboxylate groups, R-COO asymmetric stretching vibration, C-O stretching vibration, C-O-H bending of phenol groups and decreased absorption peaks of NO (NO_3^-) vibrations. Through the X-ray diffractometer there was a shift in the basal spacing d_{003} to a larger direction. Immobilization of PHBA on the surface of M /Al-LDH can be carried out using the indirect synthesis method, identified by means of FTIR spectroscopy the presence of C-C aromatic ring stretching vibrations, R-COO- asymmetric stretching vibrations, and phenolic group C-O stretching vibrations from PHBA. Adsorption kinetics model for removal on removal of $[\text{AuCl}_4]^-$ by PHBA-intercalated Mg/Al-LDH follows second-order pseudo kinetics with a constant value of $3.2778 \times 10^{-4} \text{ g/mg.min}$ while PHBA-immobilized Mg/Al-LDH follows a first-order pseudo kinetics model with a rate constant value of $1.5199 \times 10^{-2} \text{ minutes}^{-1}$. PHBA-intercalated Mg/Al-

LDH and PHBA-immobilized Mg/Al-LDH can be used to reductive adsorption process of Au (III) to Au (0) as evidenced by Au metal, which has been formed. These were seen in the stereomicroscope photo as a shiny part covering the surface of the hybrid material that turns brown. The shiny color that occurs was the reflection of the microscope light hitting the gold metal surface.

ACKNOWLEDGMENT

The financially support from the Ministry of Finance, Republic Indonesia, through the Indonesia Endowment Fund for Education (LPDP).

REFERENCES

- [1] J. M. Oh, S. H. Hwang, and J. H. Choy. "The effect of synthetic conditions on tailoring the size of hydrotalcite particles." *Solid State Ionics*, vol. 15, no. 1-4, pp. 285–291. 2002.
- [2] F. Cavani, F. Trifiro, and A. Vaccari. "Hydrotalcite-type Anionic Clay: Preparation, Properties and Application." *Catalyst Today*, vol. 11, pp. 173-301. 1991.
- [3] C.O. Oriakhi, I.V. Farr, and M.M. Lerner. "Incorporation of poly (acrylic acid), poly (vinylsulfonate) and poly (styrenesulfonate) within layered double hydroxides." *J. Mater. Chem.*, vol. 6, pp. 103. 1996
- [4] X. F. Wang, S. Q. Liu, and S. P. Li, "Methotrexatum intercalated layered double hydroxides: Statistical design, mechanism explore and bioassay study." *Materials Science and Engineering C*, vol. 49, pp. 330–337. 2015.
- [5] P.S. Braterman, Z.P. Xu, and F. Yarbberly. "Handbook of Layered Materials," in: S.M. Auerbach, K.A. Carrado, P.K. Dutta Ed. New York: Marcel Dekker Inc., 2004, pp. 373–474.
- [6] S. Chowdhury and P. Das Saha. "Comparative Analysis of Linear and Nonlinear Methods of Estimating The Pseudo-Second-Order Kinetic Parameters for Sorption of Malachite Green Onto Pretreated Rice Husk." *Bioremediation Journal*, vol. 15, no. 4, pp. 181–188. 2011.
- [7] X. F. Wang, S. Q. Liu, and S. P. Li, "Methotrexatum intercalated layered double hydroxides: Statistical design, mechanism explore and bioassay study." *Materials Science and Engineering C*, vol. 49, pp. 330–337. 2015.
- [8] J. M. Oh, S. H. Hwang, and J. H. Choy. "The Effect of Synthetic Conditions on Tailoring the Size of Hydrotalcite Particles." *Solid State Ionics*, vol. 151, no. 1-4, pp. 285–291. 2002.

- [9] G. N. Manju, M. C. Gigi, and T. S. Anirudhan, "Hydrotalcite as adsorbent for the removal of chromium(VI) from aqueous media: Equilibrium studies." *Ind. J. Chem. Technol.* Vol. 6, pp. 134–141. 1999
- [10] T. S. Anirudhan, and P.S. Suchithra., "Synthesis and characterization of tannin-immobilized hydrotalcite as a potential adsorbent of heavy metal ions in effluent treatments. *Applied Clay Science*, vol. 42, pp. 214–223. 2008
- [11] K. T. Basuki, L. A. Hasnowo, and E. Jamayanti. "Adsorption Of Uranium Simulation Waste Using Bentonite: Titanium Dioxide." *Urania-Jurnal Ilmiah Daur Bahan Bakar Nuklir*, vol. 25, no. 1, pp. 1-70, 2019.
- [12] L. A. Hasnowo. "Sintesis dan Karakterisasi Material Hibrida Mg/Al-LDH Terimobilisasi Asam Para Hidroksibenzoat." *Jurnal Forum Nuklir*, vol. 11, no. 2, pp. 81-88. 2017.
- [13] Maghfiroh. "Pengaruh Posisi Gugus Hidroksi Senyawa Turunan Asam Benzoat terhadap Pembentukan Nanopartikel Perak dari AgNO_3 ," M.A. thesis, Universitas Gadjah Mada, Indonesia, 2015
- [14] F. S. Karoonian, M. Etesami, and N. Mohamed. "Electrodeposition of Au on Reticulated Vitreous Carbon from Chloride Media by an Electrogenative Process." *Int. J. Electrochem. Sci.*, vol. 7, no. 4, pp. 3059–3071. 2012
- [15] X. Pang, M. Sun, X. Ma, and W. Hou. "Synthesis of Layered Double Hydroxide Nanosheets by Coprecipitation Using a T-Type Microchannel Reactor." *J. Solid State Chem.*, vol. 210, no. 1, pp. 111–115. 2014.
- [16] S. J. Mills, A. G. Christy, J. M. Genin, T. Kameda, and F. Colombo. "Nomenclature of the Hydrotalcite Supergroup: Natural Layered Double Hydroxides." *Mineral. Mag.*, vol. 76, no. 5, pp. 1289–1336. 2012
- [17] M.S. Frunza, D. Hritcu, and M. I. Popa. "Intercalation of Salicylic Acid into ZnAl Layered Double Hydroxides by Ion-Exchange and Coprecipitation Method." *J. Optoelectron Adv. M.*, vol. 11, no. 4, pp. 528-434. 2009.
- [18] L. Hickey, J. T. Klopprogge, and R. L. Frost. "The effect of Various Hydrothermal Treatments on Magnesium-Aluminium Hydrotalcites." *J. Mater. Sci.*, vol. 35, pp. 4347-4353. 2000.
- [19] G. Gunzler and H. I. Gremlich, *IR Spectroscopy*, Wiley-VCH: Weinheim, 2002.
- [20] S.J. Santosa, E.S. Kunarti, Karmanto, and N.A. Ikhsan. "Mg/Al layered double hydroxide anionic clay as a potential material for the remediation of acid mine leachate." *Asian J. Env. Tech.*, vol. 2, pp. 1-10. 2018.
- [21] J.T. Klopprogge, D. Wharton, L. Hickey, and R.L. Frost. "Infrared and raman study of interlayer anions CO_3^{2-} , NO_3^- , SO_4^{2-} and ClO_4^- in Mg/Al hydrotalcite." *Am. Mint*, vol. 87, pp. 623-629. 2002.
- [22] D. Wan, H. Liu, R. Liu, J. Qu, S. Li, and J. Zhang. "Adsorption of nitrate and nitrite from aqueous solution onto calcined (Mg/Al) hydrotalcite of different Mg/Al ratio." *Chem. Eng. J.*, vol. 195-196 pp. 241-247. 2012.
- [23] M. J. S. Martin, M. V. Villa, and M. S. Camazano, "Glyphosate-Hydrotalcite Interaction as Influenced by pH." *Clays Clay Miner.*, vol 47, pp. 777-783. 1999.
- [24] M. Wojnicki, E. Rudnik, M. Luty-Błoch, K. Paclawski, and K. Fitzner. "Kinetic studies of gold(III) chloride complex reduction and solid phase precipitation in acidic aqueous system using dimethylamine borane as reducing agent." *Hydrometallurgy*, vol. 127, pp. 43–53. 2012.
- [25] J. Paclawski and K. Fitzner. "Kinetics of gold(III) chloride complex reduction using sulfur(IV)." *Metall. Mater. Trans*, vol. 35, pp. 1071-1085, 2004.
- [26] K. Paclawski and T. Sak. "Kinetics and Mechanism of the Reaction of Gold(III) Chloride Complexes with Formic Acid." *J. Min. Metall., Sect. B Metall.*, vol. 51, no. 2, pp. 133–142. 2015.
- [27] H. B. Luo, H. D. and Y. Y. Xie. "Regioselective Oxidations of Phenols to o-Quinones with Dess-Martin periodenane (DMP)." *Chin. Chem. Lett*, vol. 14, no. 6, pp. 555-556. 2003.
- [28] F. C. Wu., R. L. Tseng., and R. S. Juang. "Kinetic modeling of liquid-phase adsorption of reactive dyes and metal ions on chitosan." *Water Research*, vol. 35, no. 3, pp. 613-618. 2001.
- [29] I. A. W. Tan, A. L. Ahmad, and B. H. Hameed. "Adsorption of basic dye on high-surface-area activated carbon prepared from coconut husk: Equilibrium, kinetic and thermodynamic studies." *Journal of Hazardous Material*, vol. 154, no. 1-3, pp. 337-346. 2008.
- [30] K. V. Kumar. "Linear and Non-Linear Regression Analysis for the Sorption Kinetics of Methylene Blue onto Activated Carbon." *J. Hazard. Mater.*, vol. 137, pp. 1538–1544. 2006.
- [31] K. Paclawski, and T. Sak. "Kinetics and Mechanism of the Reaction of Gold(III) Chloride Complexes with Formic Acid." *J. Min. Metall., Sect. B Metall.*, vol. 51, no. 2, pp. 133–142. 2015

- [32] S. Lagergren. "Zur Theorie der sogenannten Adsorption gelöster Stoffe." *Kungliga Svenska Vetenskapsakad. Handlingar*, vol. 24, pp. 1–39. 1898.
- [33] Y.S. Ho and G. McKay. "The kinetics of sorption of divalent metal ions onto sphagnum moss peat." *Water Res*, vol. 34, pp. 735–742. 2000.
- [34] S.J. Santosa. "Sorption kinetics of Cd(II) species on humic acid-based sorbent." *Clean–Soil, Air, Water*, vol. 42, pp. 760–776. 2014
- [35] S. J. Santosa. "Gallic and Salicylic Acid-Functionalized Mg/Al Hydrotalcite as Highly Effective Materials for Reductive Adsorption of AuCl_4^- ." *Applied Surface Science*, vol. 507 pp. 145115. 2020
- [36] R. Rusdianasari, M. Taufik, Y. Bow, and M. S. Fitria. "Application of Nanosilica from Rice Husk Ash as Iron Metal (Fe) Adsorbent in Textile Wastewater." *Indonesian Journal of Fundamental and Applied Chemistry*, vol. 5, no. 1, pp. 7-12. 2020
- [37] M. Misriyani, T. Setianingsih, and D. Darjito. "Effect of Carbonization Time of Mesoporous Carbon in the Dyes Adsorption: Rhodamine B, Methylene Blue and Carmine." *Indonesian Journal of Fundamental and Applied Chemistry*, vol. 5, no. 1, pp. 1-6. 2020
- [38] R. Mohadi, Hermansyah, P. Loekitowati, Z. Hanafiah, and H. Zulkifli. "Kinetic and Thermodynamic Study Removal of Co(II) Using Biosorbent *Spirulina* sp. in Aqueous Solution." *Indonesian Journal of Fundamental and Applied Chemistry*, vol. 2, no. 4, pp. 83-86. 2017
- [39] Krisbiantoro, P.A. "Synthesis Magnetit Asam Fulvat ($\text{Fe}_3\text{O}_4\text{-AF}$) dan Aplikasinya untuk Adsorpsi-reduksi Ion $[\text{AuCl}_4]^-$." M.A. thesis, Universitas Gadjah Mada, Indonesia, 2016.